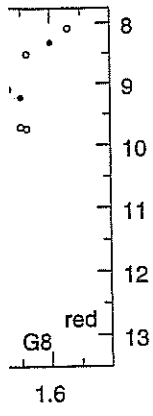


Figure 1.1 Optical spectra of main-sequence stars with roughly the solar chemical composition. From the top in order of increasing surface temperature, the stars have spectral classes M5, K0, G2, A1, and O5 – G. Jacoby *et al.*, spectral library.

The temperatures of O stars exceed 30 000 K. Figure 1.1 shows that the strongest lines are those of He II (once-ionized helium) and C III (twice-ionized carbon); the Balmer lines of hydrogen are relatively weak because hydrogen is almost totally ionized. The spectra of B stars, which are cooler, have stronger hydrogen lines, together with lines of neutral helium, He I. The A stars, with temperatures below 11 000 K, are cool enough that the hydrogen in their atmospheres is largely neutral; they have the strongest Balmer lines, and lines of singly ionized metals such as calcium. Note that the flux decreases sharply at wavelengths less than 3800 \AA ; this is called the *Balmer jump*. A similar *Paschen jump* appears at wavelengths that are $3^2/2^2$ times longer, at around 8550 \AA .



a (closed symbols)
le. Colors of giant
itudes brighter, as
N 254, 601; 1992.

th visible wave-
axies are redder,
llyptical galaxies

ould be bluer: it
in a sudden burst
ery blue; helium
inent. We would
00 Myr after star
; the deep Balmer
: of spectrum are
red million years
ber of new stars

el spectrum starts
esses, the galaxy
ical-like galaxies
d as the Universe
ninous ellipticals
terparts are a few

ty that we see in
osition. Metal ab-
llyptical galaxies:

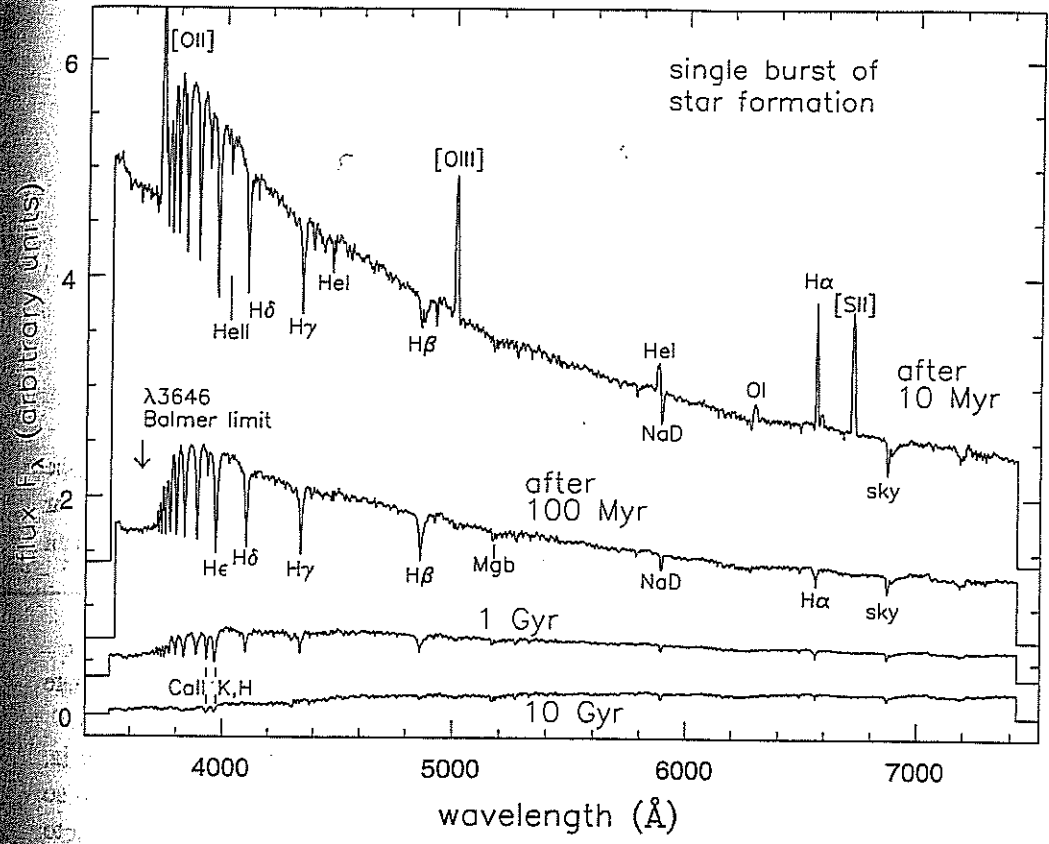


Figure 6.19 Spectra for a 'galaxy' that makes its stars in a 10^8 yr burst, all plotted to the same vertical scale. Emission lines of ionized gas are strong 10 Myr after the burst ends; after 100 Myr, the galaxy has faded and reddened, and deep hydrogen lines of A stars are prominent. Beyond 1 Gyr, the light dims and becomes slightly redder, but changes are much slower – B. Poggianti.

big ellipticals are richer in heavy elements than the mid-sized ones. The center of a galaxy is also more metal rich than its periphery: Figure 6.20 shows that the magnesium absorption is stronger, the greater the speed required for material to escape from that region of the galaxy. Smaller galaxies may have lost most of their metal-enriched gas, while larger systems were able to trap theirs, incorporating the heavy elements into new stars. Figure 1.5 showed us that metal-poor stars of a given mass are bluer, especially while they are burning helium in their cores; so we are not surprised to find that smaller galaxies with lower metal content are bluer.

The most metal-rich parts of galaxies in Figure 6.20 correspond to abundances of $1-2 Z_{\odot}$; stars at the center of luminous ellipticals are at least as metal-rich as the Sun. But they do not contain heavy elements in the same proportions as the Sun. Relatively light atoms such as oxygen, sodium, and magnesium are a few times more abundant relative to iron. We saw the same pattern in old metal-poor

they have angular
 surrounded by a low
 does indeed appear to
 peculiar morphological
 are remarkably similar to
 features are very weak, if
 ker relative to the broad
 spectrum, constructed by
 in Fig. 2.2.

l galaxies, although some
 o types of radio galaxies
 activity; broad-line radio
 re the radio-loud analogs
 ; they have a number of
 of basic phenomenology,
 ant difference is that they

ear emission-line region
 scopically, they resemble
 , [O I] λ 6300 and [N II]
 n, and might be present
 Filippenko, and Sargent
 nel of Fig. 2.1.
 often used to distinguish
 he criterion that the flux
 iver, because this flux
 VER, Seyfert-galaxy, and
 m one other on the basis
 n, Phillips, and Terlevich
 ficially similar emission-
 nguished by considering
 is of various lines are a
 herefore can be used to
 ionizing spectra. Figure
 erlevich) diagram which

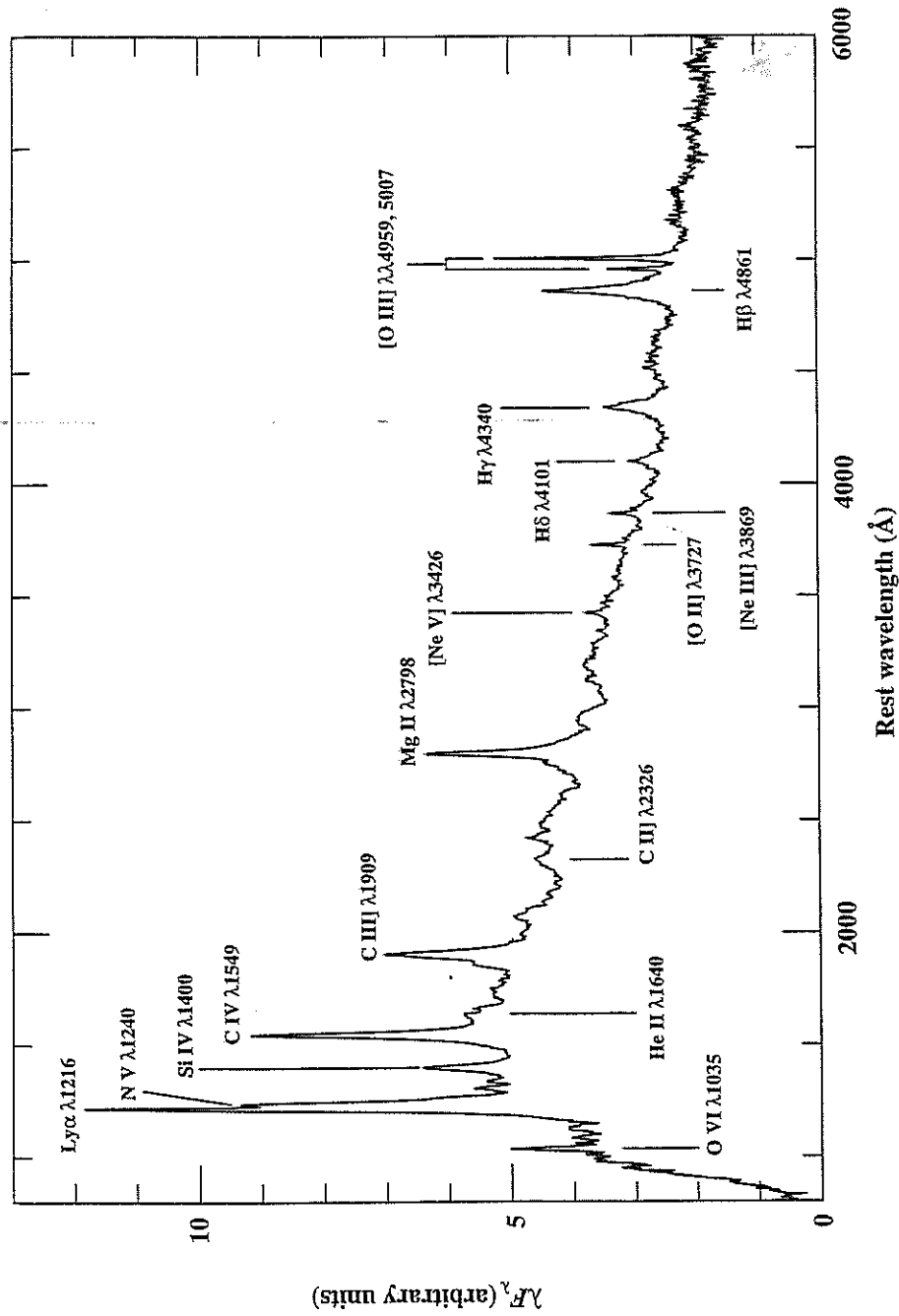
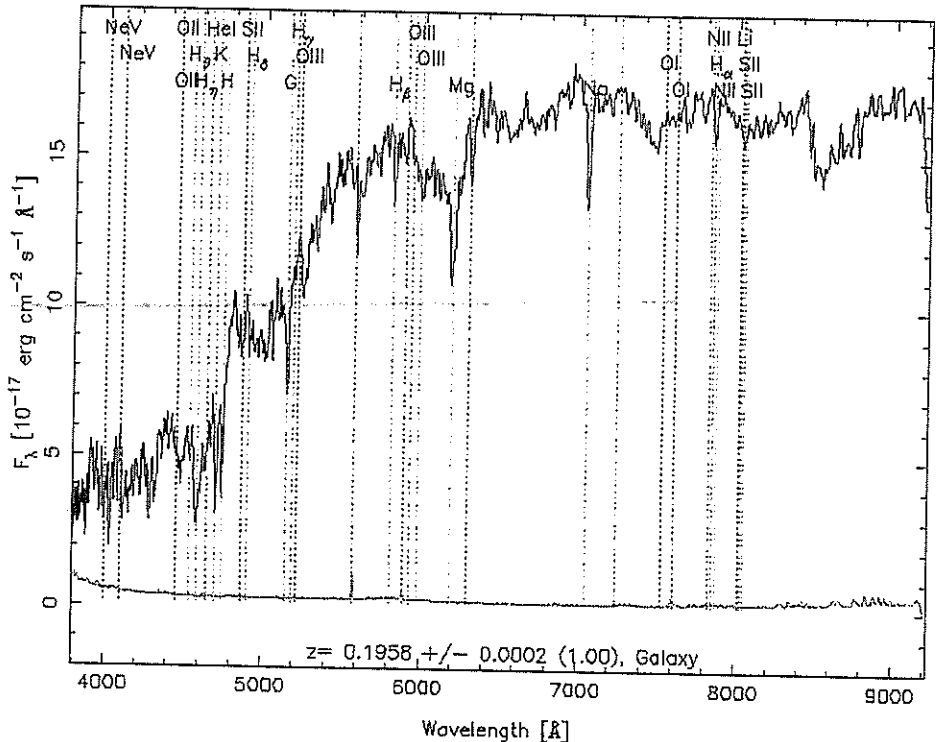


Fig. 2.2. A mean QSO spectrum formed by averaging spectra of over 700 QSOs from the Large Bright Quasar Survey (Francis *et al.* 1991). Prominent emission lines are indicated. Data courtesy of P.J. Francis and C.B. Foltz.

A1240 *redu*
 $k0 = 460$
except

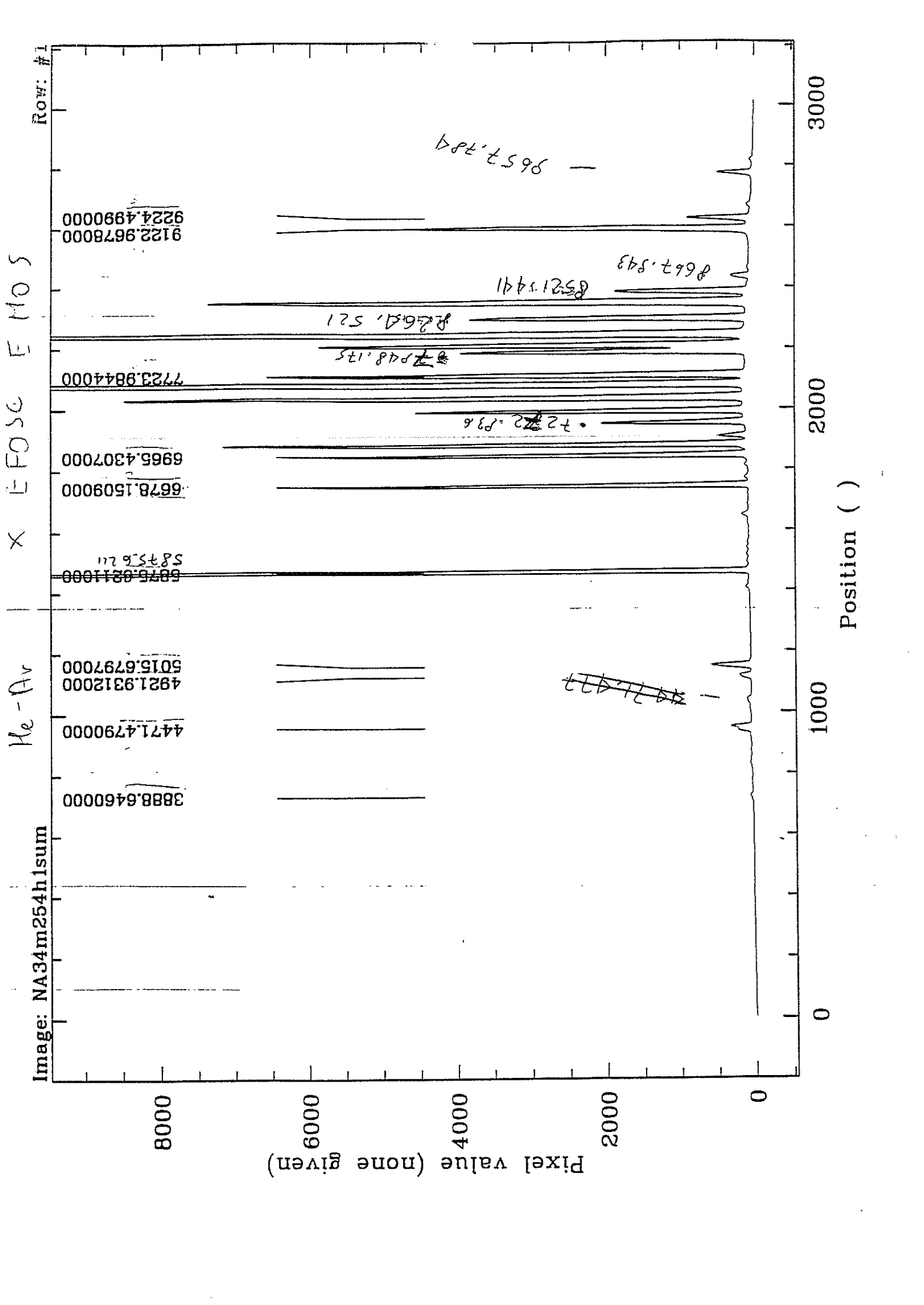
SDSS Plate 1365, MJD 53062, Rerun 26, Fiber 106

RA=170.90714, DEC=43.05779, MJD=53062, Plate=1365, Fiber=106



See the CAS Explorer page for more information on this object

File type	Directory	File name
The extracted, calibrated spectrum for this fiber, with 1d parameters	1d_26/1365/1d	spSpec-53062-1365-106.fit
Plot of the extracted, calibrated spectrum for this fiber, in gif image	1d_26/1365/gif	spPlot-53062-1365-106.gif
Plot of the extracted, calibrated spectrum for this fiber, in gzipped postscript	1d_26/1365/gif	spPlot-53062-1365-106.ps.gz
Atlas image of this object	ss_26/1365/spAtlas	spAtlas-1365-53062-106.fit
List of objects in the plate with imaging parameters	ss_26/1365	spObj-1365-53062-26.fit
Log file from the 1d data reduction	ss_26/1365	spDiag1d-53062-1365.par
The extracted, calibrated spectra for a plate	2d_26/1365	spPlate-1365-53062.fits
best fit spectroscopic classifications and redshifts	2d_26/1365	spZbest-1365-53062.fits
line fits for the spectra	2d_26/1365	spZline-1365-53062.fits
all fit spectroscopic classifications and redshifts	2d_26/1365	spZall-1365-53062.fits
Gzipped, tarred collection of spPlate and spSpec files for the plate	ss_tar_26	1365.tar.gz
A tar file with the output of the SEGUE Stellar Parameter Pipeline	sspp_26	1365-53062.tgz

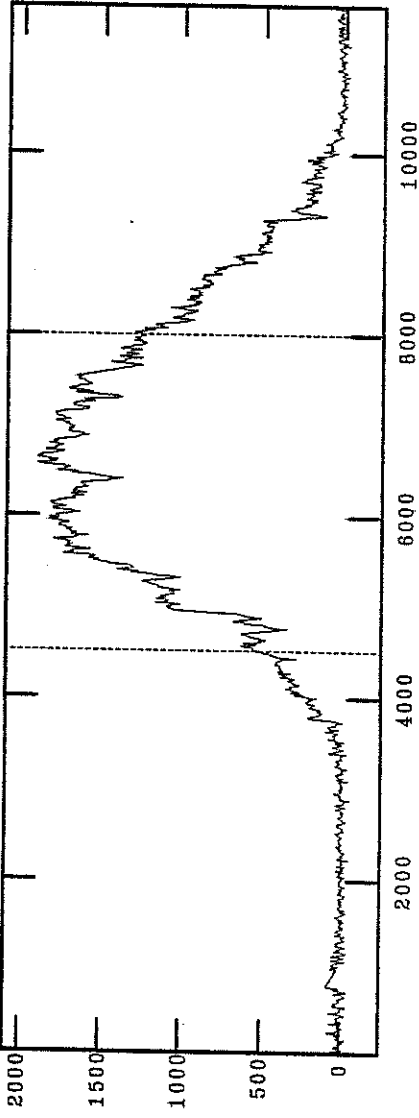


File: home\$iraf/mos4.10sals.fits HJD: 2451221.49979

1999-Feb-12 00:00:00.00

Object: EIS_0951-2 RA: 147:53:03.8 DEC: -20:47:07.9 2000.0

Object BCV: 0.000



lambda: 4519.1 8000.0

nbins: 2048x2 -em

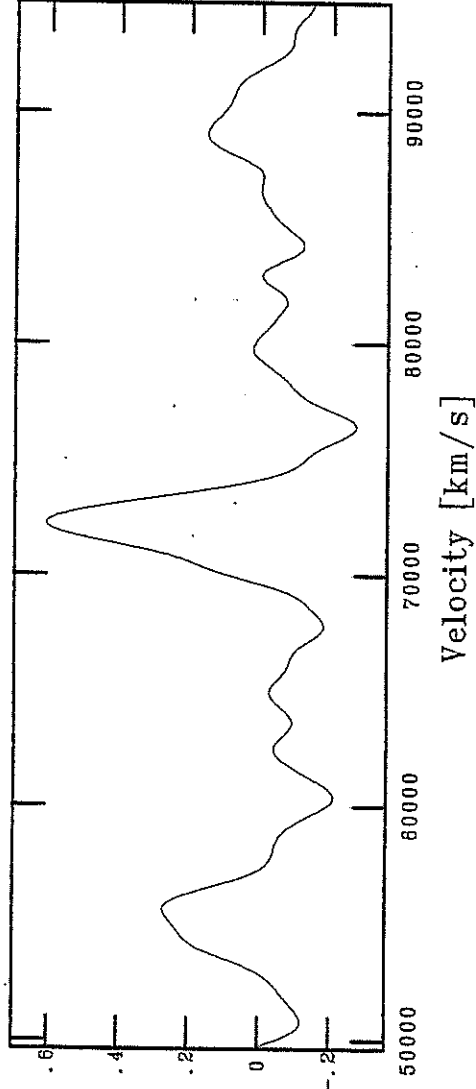
Filter: 10 20 160 280

Frac. endmask: 0.05

Template	CZ	error	R
kenn_EL	72202.9	86.068	8.85 -e
walt_sl	72306.3	120.474	8.65 -e
kenn_S0	72277.9	80.919	8.12 -e
walt_s2	72924.5	114.755	7.88 -e
kenn_Sb	72332.6	111.228	6.67 -e-f
kenn_Sa	72339.1	105.253	6.29 -e-f
m81	72481.9	99.463	6.18 -e
m31x_E	72496.7	133.548	4.51 -e
kenn_Sc	72231.7	161.633	3.00 -e-f
kenn_Ir	169524.8	318.444	2.58 -e-f

Wavelength in angstroms

1 Corr. Template: Elliptical



Velocity [km/s]

0.50-h.t. peak fit, 29 pts.

rvsao.xcsao 2.0bl7 31-Mar-1999 10:27

1999-Feb-12 00:00:00.00

File: home\$iraf/mos4.10sals.fits JulDate: 2451221.50000

Object BCV: 0.000

Object: EIS_0951-2 RA: 147:53:03.8 DEC: -20:47:07.9 2000.0

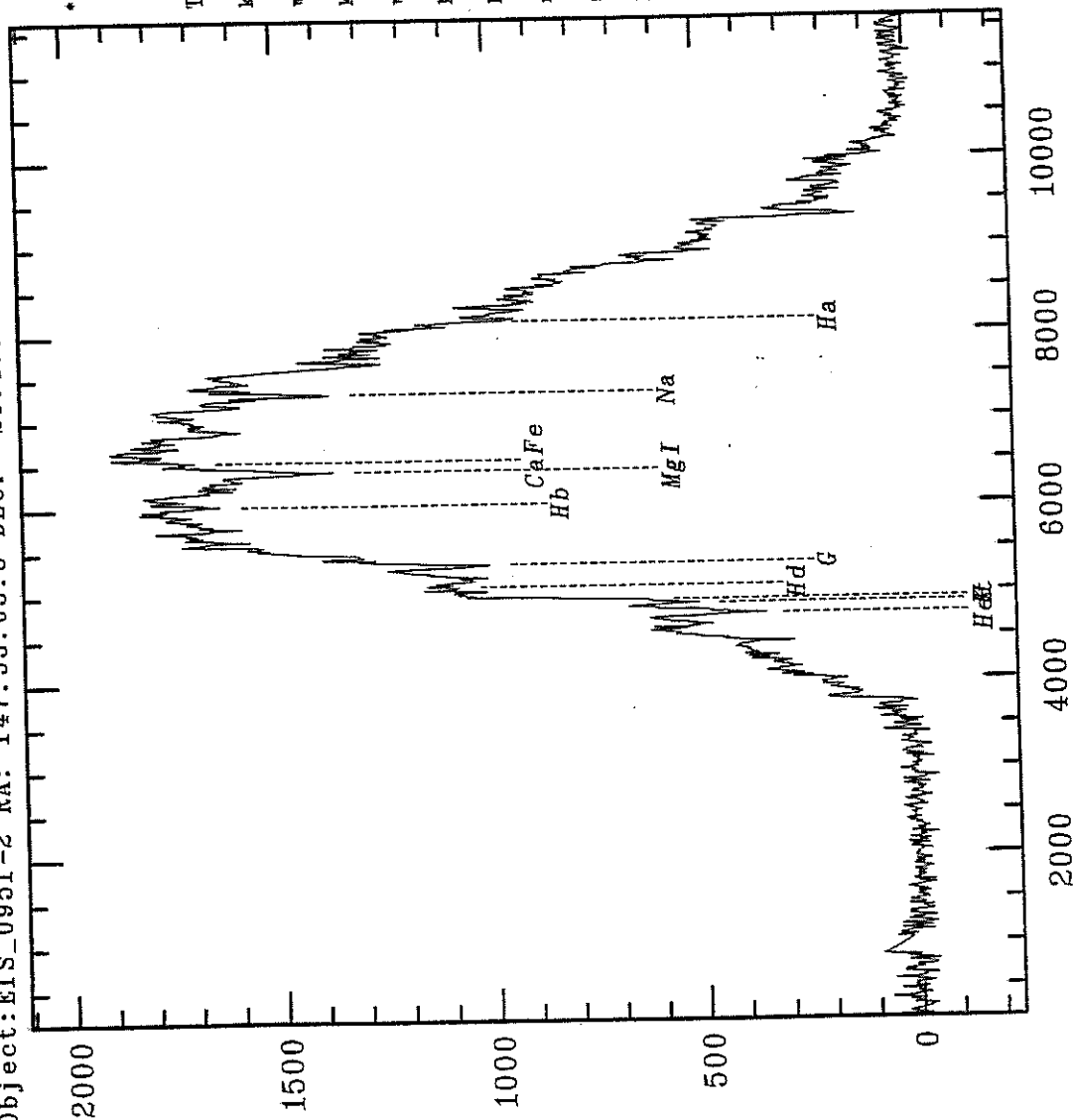
VELOCITY = 72202.95 +- 87.36 km/sec -

*Corr vel = 72202.95 +- 86.07 km/sec R= 8.85

Emiss vel = INDEF +- INDEF km/sec 0/0 lines

Template	CZ	error	R
kenn_EL	72202.945	86.068	8.85 -e
walt_s1	72306.276	120.474	8.85 -e
kenn_S0	72277.926	80.919	8.12 -e
walt_s2	72924.450	114.755	7.86 -e
kenn_Sb	72332.556	111.228	6.67 -e -f
kenn_Sa	72339.054	105.253	8.29 -e -f
mS1	72461.908	99.463	6.16 -e
mS1x_E	72496.739	133.548	4.51 -e
kenn_Sc	72331.741	161.633	3.00 -e -f
kenn_Ir	169524.76	318.444	2.58 -e -f

No emission lines found?



Wavelength in angstroms

sky (u5572i)

NOAO/IRAF V2.11.2EXPORT drsguest@suw006 Fri 10:25:43 10--Nov--2000
[skymeanx.fits]: EIS0045-2948a 3300. ap:1 beam:0

